Fourier Functional Analysis for Unsteady Aerodynamic Modeling

Suei Chin* and C. Edward Lan†

University of Kansas, Lawrence, Kansas 66045

A method based on Fourier analysis is developed to analyze the force and moment data obtained in large-amplitude forced oscillation tests at high angles of attack. The aerodynamic models for lift, drag, and pitching-moment coefficients are built up from a set of aerodynamic responses to harmonic motions at different frequencies. The final expressions for the models involve time integrals of the indicial type. Results from linear two- and three-dimensional unsteady aerodynamic theories as well as test data for a 70-deg delta wing are used to verify the models. It is shown that this modeling method is accurate in producing the aerodynamic responses to harmonic motions and the ramp-type motions.

Nomenclature

A_j	=	coefficient of cosine Fourier series
B_j	=	coefficient of sine Fourier series
C_{av}	=	average value of constant terms in the harmonic oscillation responses
C_D	=	drag coefficient
C_L	=	three-dimensional lift coefficient
C_{L_α}	=	variation of lift coefficient with respect to angle of attack
C_{L_q}	=	variation of lift coefficient with respect to pitch rate
C_m	=	pitching moment coefficient
c_l	=	two-dimensional lift coefficient
E_{ij}	=	constants associated with the zero-lag response
H_{ij}	=	constants in amplitude functions
i	=	imaginary part of a complex number
j	=	index
k	=	reduced frequency, $\omega l / V_\infty$
l	=	reference length
M	=	Mach number
N	=	number of frequencies
n	=	index for reduced frequency; index for the coefficients in Padé approximants
PD_j	=	Padé approximants
P_{ij}	=	coefficients in Padé approximants
q	=	pitch rate, rad/s
t	=	time
t'	=	nondimensional time, $t V_\infty / l$
V_∞	=	freestream velocity
α	=	variation in angle of attack, $\alpha_0 \cos kt'$
$\dot{\alpha}$	=	time rate of change in angle of attack
α_0	=	amplitude of angle-of-attack variation
α_1	=	$\alpha_m + \alpha$
α_m	=	mean angle of attack
θ	=	kt'
ξ	=	running variable in time
τ	=	dummy time integration variable

Introduction

BECAUSE of the requirement of increased performance and maneuverability, the flight envelope of a modern fighter is frequently extended to the high-angle-of-attack regime. Vehicles maneuvering in this regime are subjected to nonlinear aerodynamic loads. The nonlinearities are due mainly to three-dimensional separated flow and concentrated vortex flow that occur at large angles of attack. Accurate prediction of these nonlinear airloads is of great importance in the analysis of a vehicle's flight motion and in the design of a vehicle's flight control system. As Tobak and Schiff mentioned in Ref. 1, the main difficulty in determining the relationship between the instantaneous aerodynamic load on a maneuvering vehicle and the motion variables is that this relationship is determined not only by the instantaneous values of motion variables but also by all of the prior states of the motion up to the current state. With the advanced computing techniques, one straightforward way to solve this problem is to solve the flowfield and the flight dynamic equations simultaneously. However, this is obviously a very costly approach. In particular, at high angles of attack the aerodynamic loads depend nonlinearly on the motion variables. Under such conditions, even if the vehicles start from closely similar initial conditions, they may experience widely varying motion histories. Thus, a satisfactory evaluation of the performance envelope of an aircraft may require a large number of coupled computations, one for each change in initial conditions. Furthermore, since the motion and the aerodynamic response are linked together in this approach, there can be no reutilization of the previously obtained aerodynamic reactions.

To avoid the disadvantage of solving the coupled flowfield equations and aircraft's motion equations, an alternate approach is to use a mathematical model to describe the steady and unsteady aerodynamics for the aircraft's equations of motion. Ideally, with a mathematical model, an evaluation of the aerodynamic terms specified by the model would be required only once. The specified model can be reutilized to solve the aircraft's equations of motion over a range of motion variables and flight conditions.

In classical linear potential flow theory,[2,3] researchers in the field of aeroelasticity used the Fourier transform to relate the aerodynamic response of step change in angle of attack of a wing to that of harmonic oscillatory motions. The transient aerodynamic reaction to a step change is called the "indicial function" and has been calculated for several classes of isolated wings.[2-5] By a suitable superposition[6] of these results, the aerodynamic forces and moments induced in any maneuvers can be studied.[2,3] Tobak[7] applied the indicial function concept to analyze the motions of wings and wing-tail combinations.

Later, based on a consideration of functional, Tobak and co-workers[1,8] extended the concept of indicial function into the nonlinear aerodynamic regimes, even with aerodynamic bifurcations.[9] The simplest nonlinear aerodynamic model proposed in Ref. 1 has been applied by several authors[10-14] to perform the analysis. However, that model is accurate only to the first order of frequency and thus needs to be improved for a more general response.

Aerodynamic forces and moments acting on a rapidly maneuvering aircraft are, in general, nonlinear functions of motion variables, their time rate of change, and the history of maneuvering. How these unsteady aerodynamic forces and moments may be represented in a form suitable for flight dynamic simulation becomes uncertain, particularly at high angles of attack. For a certain type of nonlinearities produced in an experiment with small-amplitude oscillation, the analysis has been accomplished by separating the time-history data into in-phase and out-of-phase components.[15] When large-amplitude forced oscillations are employed in wind-tunnel testing at a large mean angle of attack, the aerodynamic phenomena may involve dynamic stall and/or strong vortex flow, with or without vortex breakdown. In this case, higher harmonic components in the aerodynamic response are expected to exist[16] and the phenomenon of aerodynamic lag would be important. Therefore, a more general modeling technique is needed.

In this paper a numerical method will be developed to analyze the nonlinear and time-dependent aerodynamic response to establish the generalized indicial function in terms of motion variables and their time rates of change.

Theoretical Development

In existing flight simulation two methods are commonly used to treat high-angle-of-attack aerodynamics: 1) tabulated quasisteady data[17] and 2) a local linearized model that forms a piecewise continuous fit of the nonlinear response.[18] In the present approach a formula involving time integration will be developed.

Based on functional analysis, Tobak and Schiff[1] developed a fundamental formulation of aerodynamic response for arbitrary motion. By summing incremental responses to small step changes of α and ql/V_∞ at time τ, they obtained an integral form for C_L at time t:

$$C_L(t) = C_L(0) + \int_0^t C_{L_\alpha}[\alpha(\xi), q(\xi); t, \tau]\frac{d\alpha}{d\tau}\,d\tau$$

$$+ \frac{l}{V_\infty}\int_0^t C_{L_q}[\alpha(\xi), q(\xi); t, \tau]\frac{dq}{d\tau}\,d\tau \qquad (1)$$

is obtained where ξ is over the interval 0 to τ.

To have practical applications, the functional integral form needs to be simplified. By assuming that α and q are analytical functions in the neighborhood of $\xi = \tau$, variables α and q can be expanded by their Taylor series at $\xi = \tau$. The indicial responses C_{L_α}, for example, can be expressed as

$$C_{L_\alpha}[\alpha(\xi), q(\xi); t, \tau] = C_{L_\alpha}[t, \tau; \alpha(\tau), \dot\alpha(\tau), \ldots$$
$$q(\tau), \dot q(\tau), \ldots] \qquad (2)$$

If only the first two coefficients are retained in the aforementioned Taylor series expansion, the integral form of Eq. (1) becomes

$$C_L(t) = C_L(0) + \int_0^t C_{L_\alpha}[t, \tau; \alpha(\tau), \dot\alpha(\tau), q(\tau), \dot q(\tau)]\frac{d\alpha}{d\tau}\,d\tau$$

$$+ \frac{l}{V_\infty}\int_0^t C_{L_q}[t, \tau; \alpha(\tau), \dot\alpha(\tau), q(\tau), \dot q(\tau)]\frac{dq}{d\tau}\,d\tau \qquad (3)$$

Equation (3) is applicable to the study of rapidly varying maneuvers, where hysteresis phenomena are known to exist.

However, it is difficult to implement Eq. (3). By assuming a slowly varying motion, Tobak and Schiff neglected the dependence of the indicial response on $\dot\alpha$ and $\dot q$. By further assuming that the indicial response is a function of the elapsed time $t - \tau$ instead of t and τ separately, a simplified expression of Eq. (1) can be written as

$$C_L(t) = C_L(0) + \int_0^t C_{L_\alpha}[t - \tau; \alpha(\tau), q(\tau)]\frac{d\alpha(\tau)}{d\tau}\,d\tau$$

$$+ \frac{l}{V_\infty}\int_0^t C_{L_q}[t - \tau; \alpha(\tau), q(\tau)]\frac{dq(\tau)}{d\tau}\,d\tau \qquad (4)$$

Although the form of Eq. (4) represents a great simplification over that of Eq. (1), the equation still includes the full linear form as a special case.

Jenkins[19] applied a local Taylor expansion to indicial response C_{L_α} and used that Taylor expansion form to fit numerical indicial responses calculated from a program called NLWAKE. By substituting C_{L_α} into Eq. (4), Jenkins was able to predict the oscillating motion for airfoil at low frequencies.

In the present investigation the hysteresis effect is included and the assumption of low frequencies will be removed. Therefore, an expression similar to Eqs. (3) and (4) is written as

$$C_L(t) = C_L(0) + \int_0^t [t - \tau; \alpha(\tau), \dot\alpha(\tau), q(\tau), \dot q(\tau)]\frac{d\alpha(\tau)}{d\tau}\,d\tau$$

$$+ \frac{l}{V_\infty}\int_0^\tau C_{L_q}[t - \tau; \alpha(\tau), \dot\alpha(\tau), q(\tau), \dot q(\tau)]\frac{dq(\tau)}{d\tau}\,d\tau \qquad (5)$$

In wind-tunnel testing the q effect cannot be separated from that of $\dot\alpha$. Since the method developed in this study will be used first to analyze the wind-tunnel data, $\dot\alpha$ will be used instead of q in the following investigation. The effect of $\ddot\alpha$ (i.e., $\dot q$) is included in the response without aerodynamic lag, such as the virtual mass effect in incompressible flow. Since the zero-lag response does not involve the aerodynamic lag, it is removed out of the time integral. Then Eq. (5) is rewritten for the present study as

$$C_L(t) = C_L(0) + \text{zero-lag response:}$$

$$+ \int_0^t C_{L_\alpha}[t - \tau; \alpha(\tau), \dot\alpha(\tau)]\frac{d\alpha(\tau)}{d\tau}\,d\tau$$

$$+ \frac{l}{V_\infty}\int_0^t C_{L_{\dot\alpha}}[t - \tau; \alpha(\tau), \dot\alpha(\tau)]\frac{d\dot\alpha(\tau)}{d\tau}\,d\tau \qquad (6)$$

The main objective in the present investigation is to find a suitable form for the integrand of Eq. (6). The basic building blocks of the present method are a set of aerodynamic responses to harmonic motions at different frequencies. These responses serve as a linearly independent set of functions upon which the response to an arbitrary motion can be built.

In the linear theory[2,3] the aerodynamic response can be separated into a product of an amplitude function and a phase function in harmonic motion. The amplitude function depends on motion variables and their time rate of change. On the other hand, the phase function is a function of frequency and accounts for any phase lag between the response and the excitation. In a two-dimensional linear theory the phase function is given by Theodorsen's circulation function.[2,3] After response is obtained at different frequencies with the same amplitude in harmonic oscillation, the phase function can be determined numerically. After reciprocal relations[20] have been used, the indicial function can be defined by numerical means. This approach has been used for numerical determination of indicial lift for plunging airfoils[5] and for plunging wings.[21]

The method for the linear theory is generalized as follows. Instead of assuming that the aerodynamic response is a product of an amplitude function and a phase function, it is taken to be a sum of the products of amplitude functions and phase functions in harmonic motion, i.e.,

$$C_L = C_0 + \sum_j \text{(amplitude function)}_j * \text{(phase function)}_j \quad (7)$$

In linear theory $j = 1$ in the equation. To determine the form of the amplitude functions as functions of $\alpha(t)$ and $\dot{\alpha}(t)$, and the phase functions, a functional analysis is needed. A practical method for this purpose is the Fourier analysis of forced oscillation data. The motion is assumed to be of the following form:

$$\alpha_1 = \alpha_m + \alpha_0 \cos(kt') \quad (8a)$$

$$\alpha = \alpha_0 \cos(kt') \quad (8b)$$

$$\dot{\alpha} = (-\alpha_0 k) \sin(kt') \quad (8c)$$

The first step is to Fourier analyze the response over one period. Let

$$C_L = A_0 + A_1 \cos \theta + A_2 \cos 2\theta + A_3 \cos 3\theta + B_1 \sin \theta$$

$$+ B_2 \sin 2\theta + B_3 \sin 3\theta + \cdots \quad (9)$$

From past experience,[21,22] it was found that Padé approximants provide an accurate approximation of the theoretical phase function. Therefore, Padé approximants will be used in the present model as phase functions. Following the classical airfoil theory the analysis is best performed in complex algebra. For this purpose Eq. (9) (or the experimental oscillatory results) is rewritten in a complex form as follows:

$$C_L = A_0 + (A_1 - iB_1)e^{ikt'} + (A_2 - iB_2)e^{i2kt'}$$

$$+ (A_3 - iB_3)e^{i3kt'} + \cdots \quad (10)$$

It should be kept in mind that only the real part of the response has a physical meaning. The reason for using the complex form is to benefit from the mathematical convenience of the $e^{ikt'}$ notation. If α is rewritten as

$$\alpha = \alpha_0 e^{ikt'}$$

and

$$\dot{\alpha} = (i\alpha_0 k)e^{ikt'}$$

then the classical airfoil theory suggests that the response can be put in the following form involving the products of amplitude functions and phase functions as

$$C_L \cong A_0(k)$$

$$+ E_{11}\dot{\alpha} + E_{21}\ddot{\alpha} + C_1 * (H_{11}\alpha + H_{21}\dot{\alpha}) * (1 - PD_1)$$

$$+ E_{12}\dot{\alpha}_2 + E_{22}\ddot{\alpha}_2 + C_2 * (H_{12}\alpha^2 + H_{22}\alpha\dot{\alpha} + H_{32}\dot{\alpha}^2)$$

$$* (1 - PD_2) + E_{13}\dot{\alpha}_3 + E_{23}\ddot{\alpha}_3 + C_3 * (H_{13}\alpha^3 + H_{23}\alpha^2\dot{\alpha}$$

$$+ H_{33}\alpha\dot{\alpha}^2 + H_{43}\dot{\alpha}^3) * (1 - PD_3) + \cdots \quad (11)$$

where PD are Padé approximants of order 2 and are defined as

$$PD_j = \frac{P_{1j}(ik)^2 + P_{2j}(ik)}{P_{3j}(ik)^2 + (ik) + P_{4j}} \quad (12)$$

$E_{11}\dot{\alpha}_j + E_{21}\ddot{\alpha}_j$, etc., are the zero-lag response. The variables $\dot{\alpha}_j$ and $\ddot{\alpha}_j$ are defined as

$$\dot{\alpha}_j = ik\alpha_0^j e^{ijkt'}$$

and

$$\ddot{\alpha}_j = -k^2\alpha_0^j e^{ijkt'}$$

to be consistent with higher-order terms. When $j = 1$ in the preceding equations, $\dot{\alpha}_1 = \dot{\alpha}$ and $\ddot{\alpha}_1 = \ddot{\alpha}$. In addition, H_{21}, H_{22}, H_{23}, etc., are related to the pitch rate effect. It should be noted that the terms inside the parentheses following C_1, C_2, C_3, such as $(H_{11}\alpha + H_{21}\dot{\alpha})$, represent the magnitude (or amplitude) and $(1 - PD_j)$ represents the unsteady aerodynamic lag (or phase) in response. Therefore, the present assumed form for aerodynamic modeling encompasses the classical linear theory and is capable of representing a complete set of harmonic oscillatory data with different frequencies in one expression. It should be noted that in Eq. (11) the contribution to each mode is summed in complex form. The response in time domain is given by the real part, similar to obtaining Eq. (9) from Eq. (10).

C_j are the reference values used to normalize the lift given by $A_j - iB_j$ in the least-squares error method, and j is the index consistent with the exponent of the exponential terms in Eq. (10). For example, if the j term in Eq. (11) represents the coefficient of $e^{ikt'}$, then j is 1. If the j term in Eq. (11) represents the coefficient of $e^{i2kt'}$, then j is 2, etc. The first term, $A_0(k)$, in Eq. (11) is a constant term, supposedly a function of frequency. From available experimental data for a delta wing,[22] $A_0(k)$ can be assumed to be constant approximately. The unknown coefficients P_{1j}, P_{2j}, P_{3j}, and P_{4j} are calculated from the least-squares error method. E_{11}, E_{21}, H_{11}, H_{12}, etc., are obtained separately by minimizing the sum of squares of errors. This is equivalent to a two-level optimization method to determine the unknowns in Eq. (11). That is, E, H, etc., are assumed first. Then P_{1j}, etc., are determined by minimizing the sum of squared errors. The values of E_{11}, H_{11}, etc., are varied next so that the sum of squared errors is minimized based on a gradient method. It was found that this approach is more effective in determining a global minimum solution for the unknowns than a straightforward optimization (one level) method because of nonlinearity in the unknowns in this optimization problem. It should be noted that in the literature the phase function has been typically determined by the response to plunging motions, not pitching motions. Therefore, those terms associated with $\dot{\alpha}$ in Eq. (11) do not appear. This would greatly simplify the mathematics of determining the Padé approximants. The details of the present method are discussed in the following.

Least-Squares Method

By choosing proper values of E_{11}, H_{11}, H_{12}, etc., in Eq. (11), the corresponding $A_j - iB_j$ term in Eq. (10) is then divided by the amplitude function. The result will appear as

$$V_j + iW_j \equiv 1 - \frac{A_j - iB_j - E_{1j}ik - E_{2j}(-k^2)}{\text{(amplitude function)}_j}$$

$$= \frac{P_{1j}(ik)^2 + P_{2j}(ik)}{P_{3j}(ik)^2 + (ik) + P_{4j}} \quad (13)$$

If both sides of Eq. (13) are multiplied by the denominator of the Padé approximant and separated into real and imaginary parts, then

$$\text{Re} \equiv P_{1j}k^2 - P_{3j}V_jk^2 + P_{4j}V_j - W_jk = 0 \quad (14a)$$

and

$$\text{Im} \equiv P_{2j}k + P_{3j}W_jk^2 - P_{4j}W_j - V_jk = 0 \quad (14b)$$

The sum of squared errors is defined as

$$\text{Err} \equiv \sum \text{Re}(k_i)^2 + \sum \text{Im}(k_i)^2 \quad (15)$$

By equating the first derivatives of squared errors [Eq. 15)] with respect to variables P_{1j}, P_{2j}, P_{3j}, and P_{4j} to zero, the unknown coefficients P_{1j}, P_{2j}, P_{3j}, and P_{4j} can be determined from

$$
\begin{bmatrix}
\Sigma k_i^4 & 0 & -\Sigma V_i k_i^4 & \Sigma V_i k_i^2 \\
0 & \Sigma k_i^2 & \Sigma W_i k_i^3 & -\Sigma W_i k_i \\
-\Sigma V_i k_i^4 & \Sigma W_i k_i^3 & \Sigma(V_i^2 k_i^4 + W_i^2 k_i^4) & -\Sigma(V_i^2 k_i^2 + W_i^2 k_i^2) \\
\Sigma V_i k_i^2 & -\Sigma W_i k_i & \Sigma(V_i^2 k_i^2 + W_i^2 k_i^2) & \Sigma(V_i^2 + W_i^2)
\end{bmatrix}
\begin{bmatrix}
P_{1j} \\ P_{2j} \\ P_{3j} \\ P_{4j}
\end{bmatrix}
=
\begin{bmatrix}
\Sigma W_i k_i^3 \\ \Sigma V_i k_i^2 \\ 0 \\ 0
\end{bmatrix}
\tag{16}
$$

where i varies over the range of input frequencies, and the mode subscript j on V and W has been omitted.

Gradient Method

After the unknown coefficients P_{1j}, P_{2j}, P_{3j}, and P_{4j} have been found, a one-dimensional gradient method is used to find E and H values which will make the sum of the squared errors minimum. The E or H value is perturbed first by a small amount ΔE or ΔH to find the gradient of the sum of squared errors. If the gradient tends to reduce the error, then the E or H value is perturbed further until several iterations has been reached (it is set to be 5 iterations in the current program). After that, the same procedure is applied to other E or H. Then the whole procedure is repeated again for several iterations.

Indicial Formulation

To express the aerodynamic response in time domain [Eq. (6)], the phase function, as represented by the Padé approximants, is inverted from frequency to time domains by inverse Fourier transform. The Padé approximants are first factored as follows:

$$
1 - \frac{P_{1j}(ik)^2 + P_{2j}(ik)}{P_{3j}(ik)^2 + ik + P_{4j}} = 1 - \frac{ika_{1j}}{ik + a_{3j}} - \frac{ika_{2j}}{ik + a_{4j}}
\tag{17}
$$

and then it is inverted based on a step input[2] to be

$$
\frac{1}{2\pi ik} \int_{-\infty}^{\infty} \left[1 - \frac{P_{1j}(ik)^2 + P_{2j}(ik)}{P_{3j}(ik)^2 + ik + P_{4j}} \right] e^{ikt'} \, d(jk)
$$

$$
= 1 - a_{1j}e^{-a_{3j}t'} - a_{2j}e^{-a_{4j}t'}
\tag{18}
$$

The final form for the aerodynamic response in time domain for arbitrary motion is therefore given by

$$
\begin{aligned}
C_L(t\,')C_{L\,\text{indicial}}&[t\,' - \tau, \, \alpha(\tau), \, \dot{\alpha}(\tau)]_{\tau = 0} + C_{\text{av}} + \sum_{j=1}^{m} (E_{1j}\dot{\alpha}_j \\
&+ E_{2j}\ddot{\alpha}_j) + \sum_{j=1}^{m} \int_0^{t'} \frac{d(\text{a.f.})_j}{d\alpha} * (1 - a_{1j}e^{-a_{3j}(t' - \tau)} \\
&- a_{2j}e^{-a_{4j}(t' - \tau)})\frac{d\alpha(\tau)}{d\tau} \, d\tau + \frac{l}{V_{\infty j}}\sum_{j=1}^{m} \int_0^{t'} \frac{d(\text{a.f.})_j}{d\alpha} \\
&* (1 - a_{1j}e^{-a_{3j}(t' - \tau)} - a_{2j}e^{-a_{4j}(t' - \tau)})\frac{d\alpha(\tau)}{d\tau} \, d\tau
\end{aligned}
\tag{19}
$$

where the amplitude functions (a.f.) are given by the H terms in Eq. (11), and C_{av} is the average of A_0 and is a function of α_m. It should be noted that α in Eq. (19) denotes a perturbation from α_m. The first term in Eq. (19) is the amplitude of C_L [Eq. (11)] when α is abruptly changed to $\alpha(0)$ at $\tau = 0$ and represents an initial value in the indicial lift formulation [see Eqs. (5.370) and (5.382) of Ref. 2]. Again, each mode is evaluated in complex form and the real part of the result is taken as the response in time domain.

To perform the time integration in Eq. (19), the three-point Simpson rule is used in the present method. Since the amplitude functions are determined in the frequency domain using complex algebra, for an arbitrary motion an equivalent frequency k and phase angle ϕ at τ must be obtained by matching the given α_1 and $\dot{\alpha}_1$ as follows:

$$
\alpha_1(\tau) = \alpha_m + \alpha_0 \cos(k\tau + \phi)
\tag{20a}
$$

$$
\dot{\alpha}_1 = -\alpha_0 k \sin(k\tau + \phi)
\tag{20b}
$$

Equations (20) are solved by Newton's method. It should be noted that k and ϕ are needed merely to simulate an equivalent harmonic motion in the present formulation. The resulting k
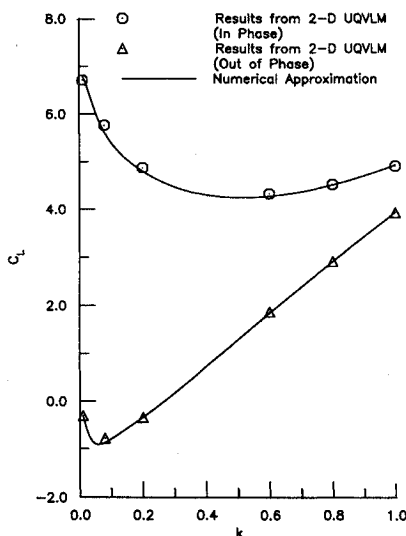

Fig. 1 Unsteady lift coefficient for a two-dimensional flat plate pitching about midchord at $M = 0.4$.
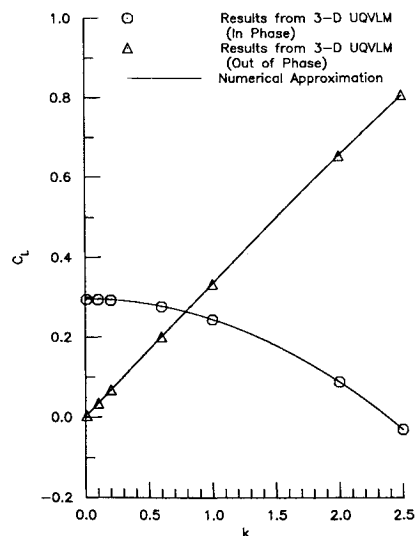

Fig. 2 Unsteady lift coefficient for a 70-deg delta wing pitching about mid-root chord at $M = 0.4$.

and ϕ are then used to determine the magnitude of the amplitude function using complex algebra.

Results and Discussion

Because appropriate high-alpha experimental data to apply the present modeling method are limited, the present method will first be tested with linear theoretical results.

Linear Results

Several cases in the two-dimensional and three-dimensional linear flow at different Mach numbers have been studied to verify the present method of aerodynamic modeling. The oscillatory two-dimensional results are computed from a two-dimensional unsteady quasi-vortex-lattice method (QVLM)[24] as input data for the current model. Through numerical experimentation, it is found that six frequencies are needed to have accurate results. In the present model [Eq. (11)], only the coefficients E_{11}, E_{21}, H_{11}, H_{21}, and P_{i1} are not zero. Three Mach numbers, 0, 0.2, and 0.4 are employed. The results at $M = 0.4$ are presented in Fig. 1. It is seen that the present modeling method is very accurate for harmonic motion. The modeling method is further verified with a 70-deg delta wing which oscillates from 0 to 20 deg in the angle of attack about the midroot chord:

$$\alpha_1 = 0.17453 + 0.17453 \cos kt' \quad \text{(in rad)}$$

This means that the mean angle of attack is 10 deg (0.17453 rad) and the amplitude of the oscillation is also 10 deg (0.17453 rad). The aerodynamic responses are calculated from a three-dimensional unsteady QVLM code.[25] Through numerical experimentation, it is found that the responses at low frequencies do not change significantly, so that accuracy in modeling would be reduced. To have more accurate approximation, high-frequency responses are needed. Seven reduced frequencies ($k = 0.01$, 0.1, 0.2, 0.6, 1.0, 2.0, 2.5) are used in
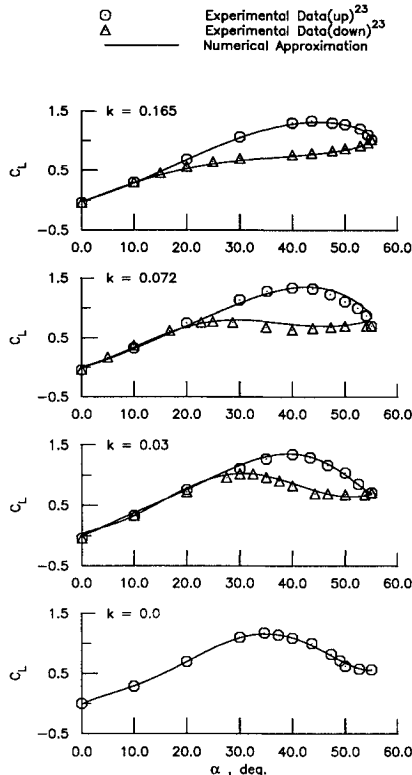
Fig. 3 Unsteady lift coefficient for a 70-deg delta wing pitching about 57% of root chord at low speed and various frequencies ($Re = 1.64 \times 10^6$).
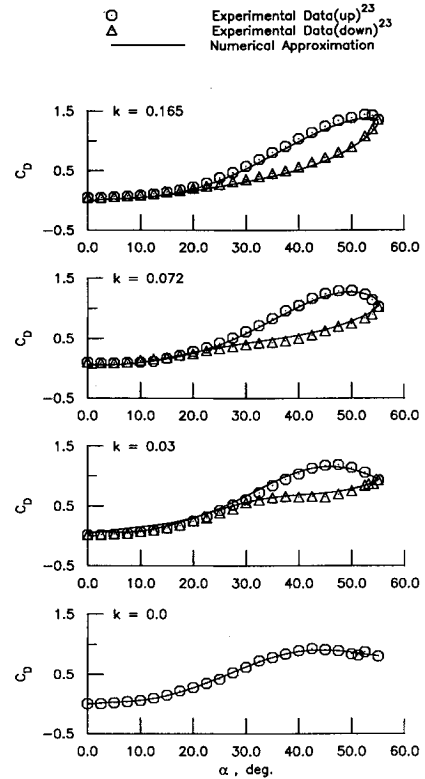
Fig. 4 Unsteady drag coefficient for a 70-deg delta wing pitching about 57% of root chord at low speed and various frequencies ($Re = 1.64 \times 10^6$).

this three-dimensional attached flow case. The results for C_L at $M = 0.4$ from modeling are plotted in Fig. 2 and again show very good agreement with results from the three-dimensional unsteady QVLM program.

Nonlinear Results

The forced-oscillation test data[23] for a 70-deg delta wing in pitching oscillation are used to validate the present nonlinear aerodynamic model. The angle of attack that describes the pitching motion is given as

$$\alpha_1 = 27.5 - 27.5 \cos kt' \quad \text{(in deg)}$$

which means the delta wing oscillates from 0 to 55 deg in angle of attack and then back to 0 deg for one cycle. The pitching center is at 57% of the root chord. k is nondimensionalized based on wing's root chord. Five sets of data corresponding to five different frequencies are available and are used as the input data to calculate the coefficients for the current aerodynamic model with five Fourier terms. The lift coefficients obtained from the aerodynamic model [Eq. (11)] are compared with the original test data in Fig. 3 with good agreement. Expressions for C_D and C_m similar to Eq. (11) are obtained with the same procedures as those used for C_L. The modeled harmonic results are compared with data in Figs. 4 and 5 for C_D and C_m, respectively. Again, the good agreement indicates that the present aerodynamic model is accurate in representing the experimental harmonic data. The coefficients for C_L are tabulated in Table 1.

To check the validity of indicial formulation [Eq. (19)] for the present nonlinear response, two oscillatory cases in Fig. 3 will be used. That is, by assuming oscillatory motion in Eq. (19), the time-integrated lift response should agree with the forced-oscillation results. The lift coefficient by integrating Eq. (19) for the same 70-deg oscillating delta wing with $k = 0.098$ is plotted in Fig. 6. Compared with the results from
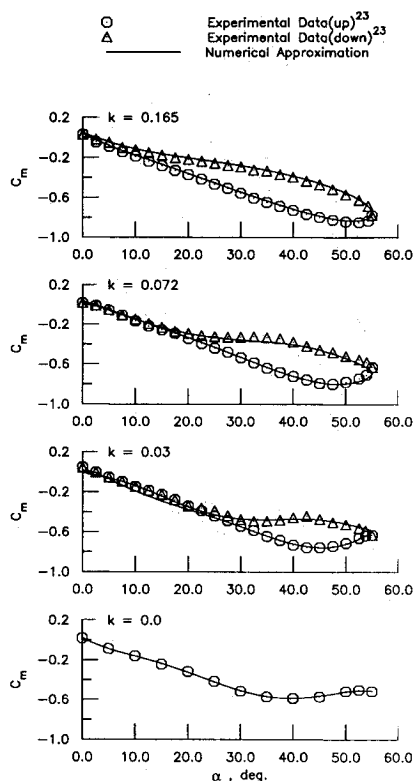
Fig. 5   Unsteady pitching moment coefficient for a 70-deg delta wing pitching about 57% of root chord at low speed and various frequencies. Moment center at 25% of root chord ($Re = 1.64 \times 10^6$).
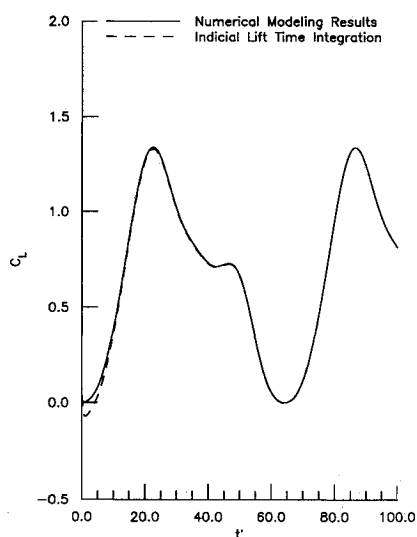

Fig. 6   Unsteady lift coefficient from numerical modeling and indicial time integration for a 70-deg delta wing in harmonic pitching oscillation about 57% of root chord at low speed ($Re = 1.64 \times 10^6$ and $k = 0.098$).

aerodynamic modeling, the integrated lift shows good agreement.

To verify the aerodynamic models further, aerodynamic responses to harmonic ramp motions for a 70-deg delta wing reported in Ref. 26 will be employed. The ramp motions start from $\alpha = 0$ to 35, 45, and 55 deg. In the present calculation based on Eq. (19), the same harmonic data shown in Figs. 3-5 and reported in Ref. 23 are used. That is, the data are based on harmonic motions from $\alpha = 0$ to 55 deg. The results for C_L are presented in Fig. 7 for a reduced frequency of 0.0714. It is seen that the present aerodynamic model is fairly accurate if the

harmonic ramp motion is from $\alpha = 0$ to 55 deg. However, the final C_L is overpredicted if the ramp motion stops at an α less than 55 deg, even though the peak C_L is still well predicted. A possible reason for this is that the harmonic data based on $\alpha = 0$–55 deg contain dynamic effect on vortex-breakdown characteristics at $\alpha < 55$ deg. Therefore, the results for C_L at a final steady $\alpha = 35$ or 45 deg should be higher.

The corresponding drag and pitching moment coefficients at one reduced frequency are presented in Figs. 8 and 9, respectively. The drag coefficient is not as well predicted in ramp motions as it is in harmonic motions (see Fig. 4). It is not known whether this is caused by differences in the test models and test Reynolds numbers. The test model for the harmonic motions (Ref. 23) has two-sided chamfered leading edges with a thickness of 0.5 in. at a Reynolds number of 1.64×10^6 based on the root chord. The model for the ramp motions (Ref. 26) is chamfered only on the lower surface of the leading edge and has a thickness of 0.25 in., and is tested at a Reynolds number of 1.54×10^6. The pitching moment coefficient appears to be well predicted except at small time.

To illustrate the present aerodynamic model [Eq. (19)] for arbitrary motions, a linear ramp motion is assumed in the
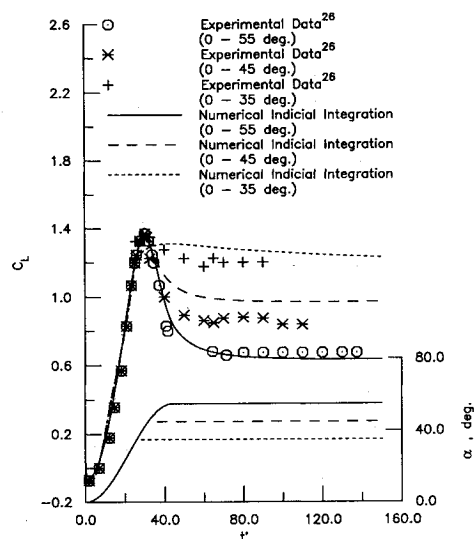

Fig. 7   Unsteady lift coefficient from indicial lift model and experiment for a 70-deg delta wing in harmonic ramp motion at low speed ($Re = 1.54 \times 10^6$ and $k = 0.0714$).
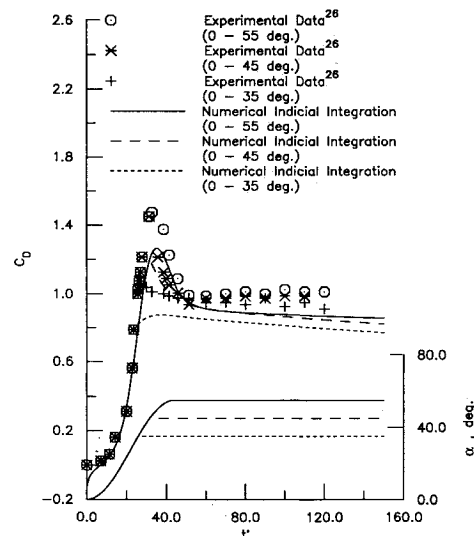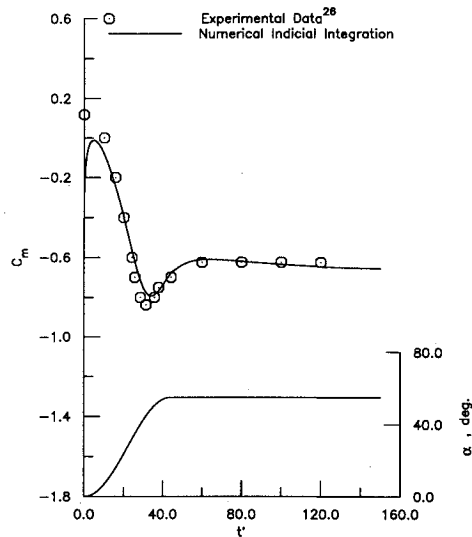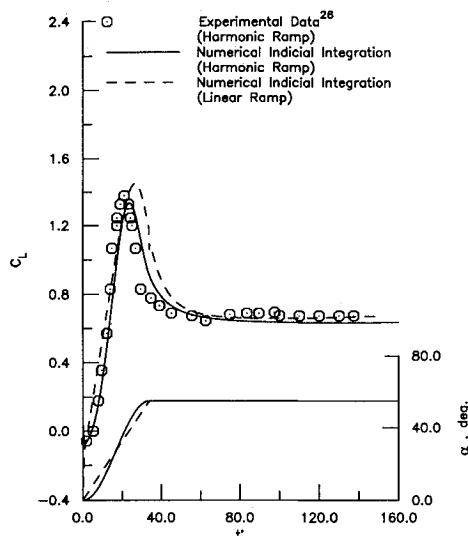

Fig. 8   Unsteady drag coefficient from indicial drag model and experiment for a 70-deg delta wing in harmonic ramp motion at low speed ($Re = 1.54 \times 10^6$ and $k = 0.0714$).

Table 1 Model coefficients for C_L for the 70-deg delta wing ($C_{av} = 0.6451$)

j	C_j	E_{1j}	E_{2j}	H_{1j}	H_{2j}	H_{3j}	H_{4j}	H_{5j}	H_{6j}
1	1.0	-0.389	1.062	0.700	0.463				
2	1.0	0.212	0.250	-0.700	0.500	0.600			
3	1.0	-0.368	0.118	-0.970	0.534	0.995	-1.019		
4	5.0	0.025	-0.063	-0.100	0.400	0.400	1.000	0.000	
5	30.0	0.186	0.039	0.096	0.588	-0.015	-0.020	0.0009	0.0007

j	P_{1j}	P_{2j}	P_{3j}	P_{4j}	a_{1j}	a_{2j}	a_{3j}	a_{4j}
1	-5.788	-0.453	5.520	0.030	-0.402	-0.646	-0.037	-0.144
2	4.947	-1.387	15.243	0.001	-1.437	1.761	-0.001	-0.065
3	3.561	0.653	4.383	0.041	0.866	-0.054	-0.053	-0.175
4	24.424	3.412	21.343	0.001	3.541	-2.396	-0.001	-0.046
5	6.127	1.604	1.244	0.025	1.545	3.379	-0.026	-0.778

Fig. 9 Unsteady pitching moment coefficient from indicial pitching model and experiment for a 70-deg delta wing in harmonic ramp motion at low speed. Moment center at 25% of root chord ($Re = 1.54 \times 10^6$ and $k = 0.0714$).

Fig. 10 Unsteady lift coefficient from indicial lift model in harmonic and linear ramp motions for a 70-deg delta wing at low speed ($Re = 1.54 \times 10^6$ and $k = 0.0926$).

integration. The results are compared with those in a harmonic ramp motion in Fig. 10. It is seen that the linear ramp motion tends to produce higher C_L values beyond the peak value because it has a higher value in $\dot{\alpha}$.

Although verification of the present model was presented only with one set of α_0 and α_m, some preliminary results with

different α_0 and α_m indicate that Eq. (19) could still produce good results if a new α-range is within the test range used in setting up the model.

Conclusions

A Fourier analysis method was developed to analyze harmonic forced-oscillation data at high angles of attack as functions of the angle of attack and its time rate of change. The resulting aerodynamic responses at different frequencies are used to build up the aerodynamic models involving time integrals of the indicial type. An efficient numerical method was also developed to evaluate these time integrals for arbitrary motions based on a concept of equivalent harmonic motion. The method was verified by first using results from two-dimensional and three-dimensional linear theories. The developed models for C_L, C_D, and C_m based on high-alpha data for a 70-deg delta wing in harmonic motions showed accurate results in reproducing hysteresis. The aerodynamic models are further verified by comparing with test data using ramp-type motions.

Acknowledgments

References

[1]Tobak, M., and Schiff, L. B., "Aerodynamic Mathematical Modeling-Basic Concepts," Dynamic Stability Parameters, AGARD-LS-114, 1981.

[2]Bisplinghoff, R. L., Ashley, H., and Halfman, R. L., Aeroelasticity, Addison-Wesley, Cambridge, MA, 1955, chaps. 5,6.

[3]Dowell, E. H. (Ed.), A Modern Course in Aeroelasticity, Sijthoff & Noordhofft, Rockville, MD, 1980, chap. 4.

[4]Heaslet, M. A., and Lomax, H., "Two-Dimensional Unsteady Lift Problems in Supersonic Flight," NACA Rept. 945, Nov. 1949.

[5]Mazelsky, B., "Numerical Determination of Indicial Lift of a Two-Dimensional Sinking Airfoil at Subsonic Mach Numbers from Oscillatory Lift Coefficients with Calculations for Mach Number 0.7," NACA TN 2562, Dec. 1951, pp. 451-453.

[6]Hildebrand, F. B., Advanced Calculus for Applications, Prentice-Hall, Englewood Cliffs, NJ, 1976.

[7]Tobak, M., "On the Use of the Indicial Function Concept in the Analysis of Unsteady Motions of Wings and Wing-Tail Combination," NASA Rept. 1188, Oct. 1954.

[8]Tobak, M., and Pearson, W. E., "A Study of Nonlinear Logitudinal Dynamic Stability," NASA TR R-209, Sept. 1964.

[9]Tobak, M., and Chapman, G. T., "Nonlinear Problems in Flight Dynamics Involving Aerodynamic Bifurcations," AGARD CP-386, Paper 25, May 1985.

[10]Katz, J., and Schiff, L. B., "Modeling Aerodynamic Responses to Aircraft Maneuvers—A Numerical Validation," Journal of Aircraft, Vol. 23, No. 1, Jan. 1986, pp. 19-25.

[11]Chyu, W. J., and Schiff, L. B., "Nonlinear Aerodynamic Modeling of Flap Oscillation in Transonic Flow—A Numerical Validation," AIAA Journal, Vol. 21, No. 1, 1983, pp. 106-113.

[12]Levy, L. L., and Tobak, M., "Nonlinear Aerodynamics of Bodies of Revolution in Free Flight," AIAA Journal, Vol. 8, Dec. 1970, pp. 2168-2171.

[13]Tobak, M., and Schiff, L. B., "Generalized Formulation of Nonlinear Pitch-Yaw-Roll Coupling, Part 1: Nonlinear Coning-Rate De-

pendence," *AIAA Journal,* Vol. 13, No. 3, 1975, pp. 323–326.

[14]Tobak, M., and Schiff, L. B., "Generalized Formulation of Nonlinear Pitch-Yaw-Roll Coupling, Part 2: Nonlinear Coning-Rate Dependence," *AIAA Journal,* Vol. 13, No. 3, 1975, pp. 327–332.

[15]Chambers, J. R., and Grafton, S. B., "Static and Dynamic Longitudinal Stability Derivatives of a Powered 1/9-Scale Model of a Tilt-Wing V/Stol Transport," NASA TN D-3591, Sept. 1966.

[16]Hanff, E. S., "Determination of Non-Linear Loads on Oscillating Models in Wind Tunnels," *IEEE 10th International Congress on Instrumentation in Aerospace Simulation Facilities,* Sept. 1983, pp. 145–151.

[17]Nguyen, L. T., Ogburn, M. E., Gilbert, W. P., Kibler, K. S., Brown, P. W., and Deal, P. L., "Simulator Study of Stall/Post-Stall Characteristics of a Fighter Airplane with Relaxed Longitudinal Static Stability," NASA TP 1538, Dec. 1979.

[18]Linse, D. J., "The Design and Analysis of a High Angle of Attack Fighter Control System," Univ. of Kansas Flight Research Lab., Rept. KU-FRL-776-1, Lawrence, KS, 1987.

[19]Jenkins, J. E., "Simplification of Nonlinear Indicial Response Models: Assessment for the Two-Dimensional Airfoil Case," *Journal of Aircraft,* Vol. 28, No. 2, 1991, pp. 131–138.

[20]Garrick, I. E., "Nonsteady Wing Characteristics," *High Speed Aerodynamics and Jet Propulsion,* Ed. by A. F. Donovan and H. R. Lawrence, Princeton Univ. Press, Princeton, NJ, 1957.

[21]Chao, C. D., and Lan, C. E., "Calculation of Wing Response to Gusts and Blast Waves with Vortex Lift Effect," NASA CR-172232, Oct. 1983.
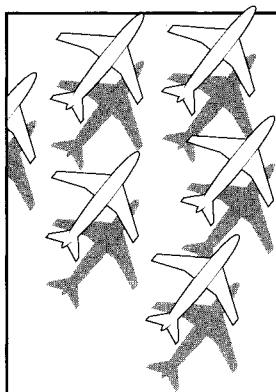
[22]Vepa, R., "Finite State Modeling of Aeroelastic Systems," NASA CR 2779, Feb. 1977.

[23]Soltani, M. R., Bragg, M. B., and Brandon, J. M., "Experimental Measurements on an Oscillating 70-Degree Delta Wing in Subsonic Flow," AIAA Paper 88-2576, June 1988.

[24]Lan, C. E., "The Induced Drag of Oscillating Airfoils in Linear Subsonic Compressible Flow," Univ. of Kansas Flight Research Lab., Rept. KU-FRL-400, 1975.

[25]Lan, C. E., "The Unsteady Suction Analogy and Applications," *AIAA Journal,* Vol. 20, No. 12, 1982, pp. 1647-1656.

[26]Bragg, M. B., and Soltani, M. R., "Measured Forces and Moments on a Delta Wing during Pitch-Up," *Journal of Aircraft,* Vol. 27, No. 3, 1990, pp. 262-267.